Thorax Online First, published on January 8, 2009 as 10.1136/thx.2008.101683

Novel Site-Specific Mast Cell Subpopulations in the Human Lung

Cecilia K Andersson[1, 2], Michiko Mori[1, 2], Leif Bjermer[1], Claes-Göran Löfdahl[1] and Jonas S Erjefält[1, 2]

[1]Dept of Respiratory Medicine and Allergology, Lund University Hospital, Lund, Sweden
[2]Dept of Experimental Medical Science, Lund University, Lund, Sweden

Corresponding author and requests for reprints should be addressed to:

Jonas Erjefält, Assoc Prof, e-mail: jonas.erjefalt@med.lu.se
Unit of Airway Inflammation, Dept of Experimental Medical Science
BMC D12, Lund University, S-22184, Lund, Sweden
Phone: +46462220960, Fax: +4646 2113417

Sources of support: The Heart & Lung Foundation, Sweden, The Swedish Medical Research Council, Swedish Asthma and Allergy Associations Research Foundation, and The Crafoord Foundation.

Running head: Novel Lung Mast Cell Heterogeneity

Key words: mast cell, alveolar, chymase, tryptase, IgE receptor.

This article has an online data supplement. Additional details on methodology are published online only at http://thorax.bmj.com

ABSTRACT

Background: Lung mast cells are stereotypically divided into connective tissue (MC_{TC}) and mucosal (MC_T) mast cells. This study tests the hypothesis that each of these subtypes can be divided further into site-specific populations created by the microenvironment within each anatomic lung compartment.

Methods: Surgical resections and bronchial and transbronchial biopsies from non-smoking individuals were obtained to study mast cells under non-inflamed conditions. Morphometric and molecular characteristics of mast cell populations were investigated in multiple lung structures by immunohistochemistry and electron microscopy.

Results: MC_T and MC_{TC} coexisted at all compartments with MC_T being the prevailing type in bronchi, bronchioles and the alveolar parenchyma. MC_{TC} were more abundant in pulmonary vessels and the pleura. Each of the MC_{TC} and MC_T phenotypes could be further differentiated into site-specific populations. MC_{TC} was of significantly larger size in pulmonary vessels than in small airway walls ($p<0.001$) while a reversed pattern was observed for MC_T ($p<0.001$). Within each MC_{TC} and MC_T population there were also distinct site-specific expression patterns of the IgE-receptor, IL-9 receptor, renin, histidine decarboxylase, VEGF, FGF, 5-Lipoxygense, and LTC_4-synthase; e.g. bronchial MC_T consistently expressed more histidine decarboxylase than alveolar MC_T ($p<0.004$). Renin content was high among vascular MC_{TC} but markedly lower among MC_{TC} in other compartments ($p<0.0002$). Notably, for both MC_{TC} and MC_T the IgE-receptor was highly expressed in conducting airways but virtually absent in alveolar parenchyma.

Conclusions: Our findings demonstrate novel site-specific sub-populations of lung MC_{TC} and MC_T at baseline conditions. This observation is suggested to have important implications in future exploration of mast cells in a variety of pulmonary diseases.

INTRODUCTION

Mast cells are multipotent cells that originate in the bone marrow and home into tissues of many organs including the lung [1-3]. They are intimately linked with allergy and have established roles in allergic rhinitis and asthma where mast cells have been extensively studied in upper and central airways, respectively [3-5]. Less is known about mast cells in more peripheral airways.

Both small airways and the alveolar parenchyma contain significant numbers of mast cells. Mast cells have in recent years been ascribed expanding roles in innate immunity, pathogen recognition, remodeling and vascular regulation [1 6-8] suggesting their involvement in a variety of non-allergic respiratory diseases like COPD, interstitial pulmonary fibrosis and pulmonary infections. *In vivo* data on human lung mast cells, particularly in peripheral regions, have however remained scarce. Most previous functional *in vivo* data come from rodents including genetically modified mice. However, apart from translational difficulties between animal models and human disease [9], mice lack mast cells in small airways and the alveolar region. Subsequently, human lung mast cell populations cannot be adequately mimicked in murine models and must be studied directly in man. In humans, however, the progress has been hampered by the enigmatic mast cell heterogeneity [3 10].

Mast cell heterogeneity, which has mainly been studied in rodents, involves differences in morphology, mediator content and histochemical characteristics as well as response to external stimuli [11 12]. Determination of the granule content of tryptase and chymase was used to identify the so called mucosal mast cells (MC_T) and connective tissue mast cells (MC_{TC}), a division that emerged as robust and became the common classification of mast cell subtypes in man [13]. This classification has also remained the archetypical division in the many excellent papers on mast cell populations in respiratory diseases [14-16]. Importantly, although MC_T is the dominating type in most parts of the lung the relative proportion and distribution of MC_T and MC_{TC} change with disease [13] with potential clinical consequences [14 17].

There are indications that division into MC_T and MC_{TC} does not adequately explain the complexity of lung mast cell heterogeneity. It is well known that the phenotype of any mast cell is highly dependent on the local microenvironment [3]. Likewise, it is known that already at healthy baseline conditions both MC_T and MC_{TC} populations are present at all anatomical compartments of the lung. Based on these notions we hypothesised that among the anatomical compartments of the lung there is a site-specific heterogeneity that is present already under non-inflamed healthy conditions and goes beyond the MC_T and MC_{TC} classification. The present study explores this possibility through detailed assessments of morphometric and molecular characteristics of lung tissue mast cell populations under base-line conditions.

METHODS

Human lung tissues

Tissue was obtained from lung lobectomy samples resected from patients undergoing surgery due to suspected lung cancer at the University Hospital in Lund, Sweden, in otherwise healthy non-smoking individuals (for patient characteristics, see table 2). Lung tissue samples were collected during a period of 5 years (from April 2001 to April 2006). Only patients with solid, well delineated tumors were included, and tissue samples were obtained far from the tumour. This procedure has commonly been used to collect human control tissue [18 19]. From each patient multiple large tissue blocks, representing the major anatomical regions of the lung, were selected for histological analysis (table 1). Central airways (bronchi), small airways (bronchioles; defined by an absence of cartilage and < 2 mm in diameter), pulmonary vessels and alveolar parenchyma were included in the analysis.

As additional control tissue we also collected bronchial and transbronchial biopsies (TBB) from young, healthy, non-atopic individuals (table 2, see also online supplement) during a study period from May 2007 to February 2008 at the Department of Respiratory Medicine, Lund University Hospital. Bronchoscopy was performed after local anesthesia with a flexible bronchoscope (Olympus IT160, Tokyo, Japan) and transbronchial biopsies were taken with biopsy forceps (Olympus FB211D) under fluoroscopic guidance in the peripheral right lower lobe, not closer than 2cm from the chest wall. Before bronchoscopy, the subjects received oral Midazolam (1mg per 10kg) and i.v Glykopyrron (0.4mg). Local anesthesia was given as Xylocain spray; local and through spray catheter. Just before the procedure, alphentanyl 0.1-0.2mg / 10kg bodyweight was given intravenously and extra Midazolam i.v. was given when needed. Central airway biopsies (n=5) were taken from the segmental or sub segmental carina in right lower and upper lobe, followed by TBB (n=5) in right lower lobe. Oxygen was given as needed under and after the procedure. Fluoroscopy of the right lung was done immediately after and 2 hours after the procedure in order to rule out significant bleeding or pneumothorax. 3-4mg betamethasone was given to prevent eventual fever reactions and the subject was discharged after 2 hours observation.
All subjects gave written informed consent and the study was approved by the local ethics committee.

Tissue processing and double immunohistochemical staining of MC_T and MC_{TC}

Immediately after excision samples for immunohistochemistry were placed in 4% buffered formaldehyde. After dehydration and paraffin embedding a large number of 3 µm sequential sections were generated from each tissue block.
A double staining protocol was used for simultaneous visualisation of MC_T and MC_{TC} cells (see online supplement for details). Briefly, after rehydration and antigen retrieval, chymase containing mast cells were detected by a primary anti-chymase antibody and a HRP-conjugated secondary antibody which was visualized using 3, 3-diaminobenzidine as chromogen. Next, the remaining MC_T subclass was visualised with an alkaline phosphatase-conjugated anti-tryptase antibody and the chromogen New-Fuchsin.

Table 1.

List of primary antibodies for mast cell related molecules with dilution, clone, manufacturer and secondary antibody.

Primary antibody	Dilution	Antigen retrieval pretreatment	Clone and Manufacturer	Secondary antibody
Monoclonal mouse anti-tryptase/AP	1:3000	-	MAB1222A, Chemicon, Temecula, CA, USA	-
Monoclonal mouse anti-chymase	1:100	MW citrate pH6	CC1, NovoCastra, Newcastle upon Tyne, UK	HRP-conjugated goat anti-mouse, Vector Laboratories, Burlingame CA, USA
Monoclonal mouse anti-interleukin 9 receptor	1:30	MW citrate pH 6	CD129, AH9R7 310402, BioLegends, San Diego, CA, USA	Horse anti-mouse IgG*, 1:200, Vector Laboratories, Burlingame CA, USA
Polyclonal rabbit anti-VEGF	1:50	MW citrate pH 6	A-20 sc-152, Santa Cruz, CA, USA	Goat anti-rabbit IgG*, 1:200, Vector Laboratories, Burlingame CA, USA
Polyclonal goat anti-5-LO	1:50	MW citrate pH 6	N-19 sc-8885, Santa Cruz, CA, USA	Donkey anti-goat IgG*, 1:100, 705-066-147, Jackson ImmunoResearch, Suffolk, UK
Polyclonal goat anti-LTC_4 synthase	1:200	MW citrate pH 6	S-18 sc-22564, Santa Cruz, CA, USA	Donkey anti-goat IgG*, 1:100, 705-066-147, Jackson ImmunoResearch, Suffolk, UK
Polyclonal rabbit anti-IgER1A	1:50	MW S1700	10980-1-AP, Proteintech group, Inc. Chicago, IL, USA	Goat anti-rabbit IgG*, 1:200, Vector Laboratories, Burlingame CA, USA
Monoclonal mouse anti-renin	1:100	MW citrate pH 6	Swant Scientific, Bellinzona, Switzerland	Horse anti-mouse IgG*, 1:200, Vector Laboratories, Burlingame CA, USA
Polyclonal rabbit anti-FGF-2	1:50	MW citrate pH 6	147 sc-79, Santa Cruz, CA, USA	Goat anti-rabbit IgG*, 1:200, Vector Laboratories, Burlingame CA, USA
Polyclonal rabbit anti-HDC	1:50	MW citrate pH 6	Kindly provided from professor Lo Persson, Lund University	Goat anti-rabbit IgG*, 1:200, Vector Laboratories, Burlingame CA, USA
Polyclonal rabbit anti-c-kit	1:400	MW citrate pH 6	Dako, Glostrup, Denmark	Goat anti-rabbit IgG*, 1:200, Vector Laboratories, Burlingame CA, USA

For antibody references see online supplement. High temperature antigen unmasking technique (microwave for 2x7 min, 800W) were performed in citrate buffer pH 6 (Merck, Darmstadt, Germany) or S1700 (Dako, Glostrup, Denmark). * Biotinylated.

Density, distribution and size analysis of MC_T and MC_{TC} populations

Mast cell density

In sections doubled stained for MC_T and MC_{TC} the density of each population was quantified manually and related to the tissue area which was determined in detail by a digital image algorithm that excluded any luminal spaces, notably also in the alveolar parenchyma (Image-pro plus, MediaCybernetics and NIS-elements, Nikon).

Size and shape analysis

In each major compartment of the lung the average cross section size was calculated for both MC_T and MC_{TC}. Cell size was measured with manual cursor tracing at high resolution digital images using software Image J (version 1.34s, National Institutes of Health, USA). MC_T and MC_{TC} were visualized in the same section by double staining (see above). The size measurements used in the main study were performed on foremost cross-sectioned airways and pulmonary vessels. To exclude any misleading results from an uneven or biased sectional plane we also analyzed cell sizes in a large numbers of longitudinally sectioned airways and vessels. To further improve our quantification of mast cell sizes we employed a stereological approach using volume fraction measurements from a fixed cell number quantification[20]. In short, using a point grid overlaid onto randomly orientated tissue sections point counting was performed until a fixed numbers of mast cells (240 /patient) had been hit by one or more points. With similar cell numbers analyzed differences in volume fraction will equate differences in mean cell size. The volume fraction for each mast cell subtype and compartment was calculated using the equation:

$$V_{V\,(MC,compartment)} = \frac{\Sigma P\,(MCT,MCTC)}{\Sigma P\,(SA,PV)}$$

Where P is points counted, SA denotes the small airways compartment and PV is pulmonary vessels. The cell shape was calculated using the formula: $circularity = 4\pi\,(area/perimeter^2)$.

Immunohistochemical identification of mast cell-related molecules

Triple staining with immunofluorescence was used to simultaneously visualise both MC_{TC} and MC_T populations together with the following mast cell-related molecules: IgE receptor (IgεR1α), histidine decarboxylase (HDC), IL-9 receptor (IL-9R), vascular endothelial growth factor (VEGF), 5 lipoxygenase (5-LO), leukotriene C_4 synthase (LTC_4-S), renin and fibroblast growth factor (FGF-2) (see online supplement and table 1 for protocol details). The markers was selected to represent multiple aspects of mast cell biology ranging from mast cell-promoting/survival factors (c-kit/CD117, IL-9R), key activators (IgER1A), key enzymes used to produce mast cell-derived eicosanoids (LTC4-S and 5–LO) and histamine (HDC), as well as growth factors previously described in mast cells (e.g. VEGF and FGF). After appropriate antigen retrieval, sections were stained for the molecule of interest using specific and validated primary antibodies (table 1) and visualised by an appropriate biotinylated secondary antibody and Alexa-Flour 555-conjugated streptavidin (Molecular Probes, OR, USA). Next, MC_{TC} and MC_T cells were stained by anti-tryptase and anti-chymase antibodies that were labelled (Zenon® IgG labelling kit) with AlexaF-488 and AlexaF-350 fluorochromes, respectively.

Transmission electron microscopy

From each lung compartment separate glutaraldehyde/formaldehyde-fixed samples were processed and analysed by routine transmission electron microscopy using a standard protocol[21] and a Philips CM-10 TEM microscope (Philips, Netherlands). Mast cell subtypes and ultrastructural signs of degranulation were analysed according to previously described ultrastructural criteria [21].

Quantifications and statistics

For direct comparison of the lung compartments within each single section the main quantifications were, if not stated otherwise, performed on large sections from the surgical material. For quantification of mast cell-related molecules and morphometric parameters numerous mast cells were analyzed in three separate tissue blocks from each patient, selected to contain

the major anatomical compartments. When possible we also corroborated our findings in bronchial and transbronchial biopsies from young healthy individuals.

Data were analysed statistically using Mann Whitney rank sum test for comparison between two groups when overall significant difference was detected, and one-way ANOVA corrected for Bonferroni's Multiple Comparison Test for comparison between three groups or more using GraphPad Prism v. 4.03, GraphPad software, Inc. Differences between groups were considered significant at $p \leq 0.05$.

RESULTS

Table 2.

Subject Characteristics and Overview of Tissue Samples

Variable	Lung resections	Bronchial biopsies	Transbronchial biopsies
Patients (n)	10	5	
Tissue block/biopsies	n=28*	n=26	n=28
Males/females	2/8	4/1	
Age (years)	61.9 (33-76)	29.6 (25-41)	
FEV_1 % of predicted	110 (82-141)	107 (95-116)	
Smoking (pack years)	0	0	

Data presented as median values and ranges. *Each large tissue block from the resections were selected to represent the major anatomical lung compartments

MC_T and MC_{TC} are abundant at all airway levels with a gradual increase towards peripheral regions.

Mast cells were abundant at all airway levels (figs 1 A and 2A-E) with a gradual and statistically increased density towards the alveolar parenchyma (fig 1 A). Mast cells were also abundant in the adventitial layer in pulmonary vessels and in the perivascular layer outside the adventitia (figs 1A and 2B, E) whereas the numbers in the pleural wall was modest (26.7±5 cells/mm^2). Similar MC densities were present in bronchial and transbronchial biopsies from young healthy controls.

Proportion and distribution of MC_T and MC_{TC}

Lung tissues double stained for MC_{TC} and MC_T revealed that in all major anatomical compartments, except in the adventitia of pulmonary vessels, MC_T was the predominant subtype (fig 1A-B). The proportion of MC_T was highest in conducting airways, slightly elevated in the alveolar parenchyma, and significantly decreased in pulmonary vessels (fig 1B). MC_{TC} were the most numerous subtype in the pleural wall, with 20.5±7 cells per mm^2, compared to 6.2±2 cells per mm^2 for MC_T ($p<0.0001$). Details on MC_{TC}/MC_T distribution within subcompartments in conducting airways and vessels are presented as online supplementary data.

MC_T and MC_{TC} may be divided into further site-specific subgroups.

Differentially sized MC_T and MC_{TC} populations in distinct anatomical compartments

By measuring cell cross section areas it was revealed that the size within each of the MC_T and MC_{TC} population differed dramatically between anatomical regions (fig 3A). Large MC_T cells were found in bronchi and small airways and significantly smaller MC_T were present in pulmonary vessels ($p<0.001$). For MC_{TC} a reverse pattern were found, i.e. large MC_{TC} in pulmonary vessel walls, and a significantly ($p<0.001$) smaller MC_{TC} population in bronchial and small airway walls (fig 3A). To exclude that the size differences were not caused by an uneven tissue orientation in distinct MC populations equally manifested differences was present

in strictly longitudinally sectioned airways and vessels (see online supplement). Distinct size changes were further corroborated by stereology where distinct volume fractions were present after analysis of equal mast cell numbers. In small airways the volume fraction of MC_T and MC_{TC} was 0.027±0.004 and 0.009±0.0007 (p=0.0003), respectively. For pulmonary vessels the opposite was true. MC_T had a smaller (p=0.0019) volume fraction per mast cell number (0.009±0.0008) compared to MC_{TC} (0.019±0.002).
In alveolar regions mast cells displayed similar alterations as conducting airways; i.e. large MC_T and smaller MC_{TC} (fig 3A). The distinctly sized mast cell population was in all compartments confirmed also after labelling of the mast cell surface marker c-kit (CD117).

Shape Index
Calculating of the circularity of MC_{TC} and neighbouring MC_T cells showed that MC_{TC} cells were significantly more circular in all compartments (apart from the alveolar parenchyma) compared to neighbouring MC_T cells in the bronchial wall (p=0.008), small airways (p<0.001), and pulmonary vessels (p=0.004), fig 3B-E). Occasional MC_T cells in bronchi and small airways had a dendritic morphology (fig 3C-E).

Confirmation of non-degranulating phenotypes by electron microscopy
Ultrastructural examinations of MC_{TC} and MC_T subtypes, which were identified by their distinct granule morphology[21], revealed that at all examined compartments mast cells were of a non-degranulating phenotype i.e. displaying filled granules lacking classical ultrastructural sign of e.g. anaphylactic or piecemeal degranulation.

Distinct expression of mast cell-related molecules in site-specific MC_T and MC_{TC} populations.
Distinct differences within each MC_T and MC_{TC} population could be further corroborated by differential molecular expression of mast cell-related molecules (table 1, data summarised in fig 4A-B). Thus, apart from the expected differences between MC_{TC} and MC_T cells, our data reveal multiple examples of site-specific expression patterns within each of the MC_{TC} or MC_T populations (figs 4-6).

MC_{TC}: On the whole, alveolar MC_{TC} had a low expression of the present set of mast cell-related molecules compared to e.g. vessel and airway MC_{TC}. The populations of MC_{TC} in bronchi, small airways, and alveolar walls differed dramatically in their expression of IgεR1α (fig 4 C). There was a significant and gradual decrease from an extensive IgεR1α expression in bronchi (71.2±6%), moderate in small airways (43.4±10%), to a virtually absent expression among alveolar MC_{TC} cells (fig 4B-C). A similar pattern was seen in bronchial and transbronchial biopsies from our young control population. The expression of HDC followed the same pattern as the IgεR1α. HDC expression significantly decreased from bronchi and small airways (60.6±5 and 65.5±5, respectively) to the alveolar region (41.2±3%, p=0.002, fig 4D). Renin, just recently discovered as an airway mast cell mediator [8], had significantly (p=0.002) elevated expression in the large-size MC_{TC} of pulmonary vessels (65.6±7%) compared to the small-size MC_{TC} populations found in other compartments of the lung (figs 4B and 5B). Notably, expression of the leukotriene producing enzymes 5-LO and LTC_4-S were foremost expressed in the MC_{TC} populations of pulmonary vessels and small airways (figs 4B and 5 E-F). For example, the MC_{TC} 5-LO expression in small airways (86.8±7%) and pulmonary vessels (82.1±14%) were increased compared to central airways (15.6±15.6%, p=0.017 and 0.03, respectively) or the alveolar parenchyma (12.8±12.8%, p=0.008 and 0.021, respectively). A similar heterogeneity was also observed for the IL-9R among the lung MC_{TC} populations (figs

4B and 5 A). Notably, as for renin, VEGF and FGF2 were absent among the alveolar MC_{TC} (fig 5 C-D).

MC_T: Also the MC_T differed significantly in their expression pattern between the different parts of the lung. The proportion of MC_T expressing IgεR1α was, in similarity to MC_{TC}, highest in bronchi (72.5±7%), significantly decreased in small airways (43.0±10%, p=0.05) and virtually absent in the alveolar region (4.7±2%, p=0.0002, fig 4 A, C). The proportion HDC expressing MC_T also followed the MC_{TC} expression with a decrease from bronchi to the alveolar region (75.4±2 to 14.4±4%, p=0.004, fig 4D). Although renin was expressed in the central airways (21.4±1%) the proportions of renin-positive MC_T were increased in more distal airways (small airways: 51.5±10% p=0.05, alveolar region 58.5±9% p=0.0006, fig 5B). A similar pattern was observed for 5-LO, with a low bronchial expression (10.1±3%) compared to e.g. small airways and pulmonary vessels (32.6±7% and 46.7±15%, respectively: p=0.0173, fig 5F). In contrast, LTC_4-S was richly expressed in the central airways (53.4±4%, fig 5E). Both FGF-2 and VEGF were richly expressed in the central airways and pulmonary vessels with only a moderate decrease in small airways and alveolar tissue (fig 5 C and D).

DISCUSSION

The phenomenon of mast cell heterogeneity has been known for decades and studied in several species [3 10 22]. Yet, apart from the MC_T and MC_{TC} classification this phenomenon has remained poorly investigated, especially under human *in vivo* conditions. The present work describes a new level of heterogeneity by showing that already under base-line conditions each anatomical compartment of the lung contains distinct MC_T and MC_{TC} populations. For example, the frequently studied and highly IgεER1α-expressing MC_T population in bronchi and small airways differ markedly, both in size and molecular content, from the less studied MC_T populations in alveoli or pulmonary vessels. Equally striking differences occurred between site-specific MC_{TC} populations. These findings point out mast cells as exceedingly plastic cells with a baseline phenotype determined by the local tissue milieu.

The present type of novel heterogeneity has several practical implications. In agreement with previous studies [14 16 17] this report suggests that quantification of lung mast cells in disease without proper information of anatomical location or subtype may be misleading; a certain subtype in one location may display increased numbers and/or activation whereas the situation may be reversed in neighbouring areas. An additional aspect underscored by this study is the complexity in assessing lung-derived mast cells *ex vivo.* Indeed, from our data it can be expected that purification of mast cells from lung homogenates yield a mixture of several populations with potentially different propensity to survive and get activated *ex vivo*. This type of heterogeneity may account for the many previously reported discrepancies in functionality among lung-derived mast cells. In this context knowledge about the present site-specific heterogeneity may be helpful if lung mast cells were instead purified from dissected well-defined compartments of the lung together with e.g. CD88-based separation of MC_T and MC_{TC} proportions [23].

In this study, mast cells were plentiful at all regions of the lung and, in consistence with other studies [12 24], MC_T was by far the most abundant subtype. Previous studies have shown an increase in mast cell density in small airways compared to bronchi [15 16]. Much less have been known regarding alveolar mast cells. Interestingly then, in this study the alveolar lung parenchyma stood out as the most mast cell-rich compartment. In light of this, the present novel finding of a paucity of IgεR1α on alveolar mast cells is intriguing and suggests a reduced capacity for classical anaphylactic degranulation among alveolar mast cells. In agreement, Balzar *et al*. report in passing of reduced IgE-bearing mast cells in the alveolar tissue of asthmatics and healthy controls [25]. It seems rational to have mechanisms for local down regulation of FcεRI [26] and thus prevent an anaphylactic degranulation in alveolar regions. Common effects of classical degranulation like plasma extravasation would be a catastrophic event in the alveoli. It is thus likely that alveolar mast cells is under strict regulation by non-IgE mast cell triggers e.g. C5aR, CD30L etc. [23 27]. Irrespective of activation mechanism, alveolar mast cells are likely to have a variety of roles ranging from regulation of blood flow, a notion supported by the present high renin content in alveolar mast cells, to participation in the many new functions recently ascribed to mast cells, ranging from immune modulators, effector cells in innate immunity to pro-fibrotic cells [6 28-30].

Size differences between mast cell populations *in vitro* has been reported [31 32] but no link has been made to an *in vivo* setting. Our extensive quantification of MC size, with data from both cross- and longitudinally sectioned airways and vessels, would yield a fair estimation of the size of MC_T and MC_{TC} since we did not assume about the orientation, used randomly orientated tissues, counted nucleated cells only, and as we counted all MCs in each analyzed struc-

ture. Non-biased stereology is nevertheless the best approach for measure cell density and size[20 33]. However, many practical limitations exist in incorporating these methods into clinical studies, due to e.g. limited quantity of tissue samples and that studies using human material cannot be completely designed to fulfil stereological criteria. The most correct way to measure individual cell size would be with the optical dissector method. After the present double immunohistochemical staining of MC_T and MC_{TC} populations, this was however not applicable. Taking advantages of the fact that that the present tissue blocks were randomly selected and oriented, we therefore applied the stereology approach 'volume fraction' that confirmed our conventional cell area measurements[20 34].

The observation in this study of site-specific size differences among MC_T and MC_{TC} populations represents an intriguing and novel finding. These differences were consistent regardless of whether the size determination was based on visualisation of granule proteins or surface markers. Any shape and size changes due to degranulation were ruled out since our electron microscopic analysis showed that the mast cells were resting irrespective of their localisation. Currently it is unknown how one part of a tissue selectively can promote the growth of one mast cell subtype while suppressing the other. Speculatively, one explanation could be presence of site-specific growth factors that act differentially on newly recruited MC_T and MC_{TC} progenitors [2 35]. Although it is difficult to speculate about the biological significance of distinctly sized populations, the consistency of this feature could be a useful discriminator in the further characterization of site-specific populations. Some clues about functional roles is however provided by Schulman *et al* who reported a differential histamine release among differently sized mast cell populations *in vitro*[36].

From a more general perspective our discovery of site-specific mast cell subtypes supports the idea of microlocalization as a determinant in creating differential phenotypes of infiltrating cells [37]. Indeed, both the airways and pulmonary vessels contain sub-anatomical compartments such as smooth muscle bundles and epithelial/endothelial regions that may differentially attract and/or alter mast cell behaviour [16 17 38-40]. Hence, the fact that pulmonary vessels, conducting airways and alveoli contain different proportions and types of structural cells may in part explain the present novel site-specific mast cell populations.

Apart from the classical staining for tryptase and chymase the mast cells in the present study was assessed for a variety of other mast cell-related molecules. By this approach we could demonstrate several statistically significant differences within each of the MC_T and MC_{TC} categories. Some of them are intriguing, like the reduced IgεR1α and increased renin expression in the alveolar region. Others are at the current state difficult to assign any specific functional consequence but they nevertheless strongly support our hypothesis of site-specific mast cell populations. Importantly, for our immunohistochemical staining we used large sections that contained all anatomical compartments. This guaranteed that our comparison of molecular expression was done between anatomical regions subjected to exactly the same immunohistochemical conditions. Further, electron microscopy confirmed that the mast cells were of a non-degranulated phenotype. Hence, the present differences in mediator content or receptor expression are not caused by differential degranulation but rather reflect distinct molecular expression at resting base-line conditions. One interpretation of this is that the unique molecular milieu in each anatomical compartment gives rise to differential mast cell priming reflecting the different needs and functions of mast cells in various parts of the lungs.

In summary, the present study discloses several novel aspects of the heterogeneity of normal lung mast cells. Many of them clearly go beyond the prevailing MC_T and MC_{TC} classification. As revealed by morphological and molecular parameters, small and large airways, pulmonary vessels, and the alveolar parenchyma seem each of them to harbour site-specific MC_T and MC_{TC} populations. Among these the alveolar mast cell types comprised the most abundant yet most poorly studied populations. Consideration of the present expanded heterogeneity seems warranted in future studies on physiologic and pathogenic roles of mast cells in health and respiratory disease.

ACKNOWLEDGEMENTS

We thank Karin Janser and Britt-Marie Nilsson for skilful technical assistance with tissue processing, immunohistochemical staining and TEM procedures. We also thank Professor Lo Persson for kindly providing the HDC antibody.

Funding

This study was supported by grants from The Heart & Lung Foundation, Sweden, The Swedish Medical Research Council, Swedish Asthma and Allergy Associations Research Foundation, and The Crafoord Foundation.

Competing interests: None.

LEGENDS

Figure 1. Mast cell density in healthy human lung. The density was significantly increased from central to distal airways. Total mast cell density, as well as the number of MC_T and MC_{TC} was analysed per mm^2 lung tissue in central airways, small airways, alveolar parenchyma and the adventitia and perivascular tissue of pulmonary vessels (A). The proportion of each subtype (%) for each compartment is shown in B. Pictures C and D illustrates the detailed localisation in % of mast cell subtypes in small airways and pulmonary vessels, respectively. Data expressed as mean ± SEM. *p<0.05 compared with total mast cells in central airways. $^{\#}$p<0.05, $^{\#\#}$p<0.01 compared with MC_{TC} in pulmonary vessels. Statistical analyses were performed using Mann-Whitney rank sum test.

Figure 2. Representative micrographs of immunohistochemical staining (new fuchsin - red) of tryptase positive mast cells in different anatomical compartments of the lung, (A) bronchi with high-magnification image of immunohistochemical staining of MC_T (red) and MC_{TC} (brown) highlighted as insert, (B) small airways, (C) alveolar parenchyma, (D) high magnification of a mast cell in the alveolar septa, (E) pulmonary vessels, and (F) ultrastructural TEM image of a mast cell (MC) in close proximity to a type II pneumocyte (PII) situated in the alveolar septa. Inset in F shows the characteristic scroll lattice of a resting MC_T granule. The background tissue is outlined by differential interference contrast (DIC) microscopy. Bar = 50 μm for A, B, C and E. Bar = 10 μm for D. Bar = 1 μm for F and 250 nm for magnification of mast cell granular scroll.

Figure 3. Mast cell size and shape analysis in different lung compartments. (A) Size alterations for MC_T and MC_{TC} in central airways, small airways, alveolar parenchyma and pulmonary vessels. (B) Shows differences in shape (circularity) between and within MC_T and MC_{TC} in central airways, small airways, and pulmonary vessels. No significant shape difference was found in alveolar parenchyma. Results are shown as scatter plot graphs were black bar indicates mean. Representative photomicrograph exemplifying the variation of mast cell shapes, showing from left to right, two examples of highly irregular “dendritic” mast cells (C-D) and more circular types (E), stained for c-kit. Bar = 10 μm. Statistical analyses in A-B were performed using Mann-Whitney rank sum test when comparing two groups and one-way ANOVA corrected for Bonferroni's Multiple Comparison Test for comparison between three or more groups. Significant differences when comparing MC_T and MC_{TC} in different compartments: *p<0.05, ***p<0.001. $^{\#\#\#}$p<0.001 is considered significant when comparing MC_T size between anatomical locations.

Figure 4. Summary of molecular staining patterns shown as relative expression (%) of mast cell related molecules within MC_T (A) and MC_{TC} (B) in different lung compartments. The proportion of total mast cells and MC_T and MC_{TC} subtypes staining positively for IgE and histidine decarboxylase, HDC is shown in C and D, respectively. Data expressed as mean ± SEM. *p<0.05, **p<0.01, ***p<0.001 compared with total mast cells in central airways. $^{\#}$p<0.05 compared with MC_T in small airways. $^{¤}$p<0.05, $^{¤¤}$p<0.01 compared with MC_{TC} in small airways. Statistical analyses were performed using Mann-Whitney rank sum test.

Figure 5. Molecular expression pattern (%) of (A) IL-9R (B) renin, (C) VEGF, (D) FGF-2, (E) LTC_4S and (F) 5-LO in different compartments. Results are shown as the percentage of total mast cells, and MC_T and MC_{TC} subtypes, that are positive for the respective mediators. Data expressed as mean ± SEM. *p<0.05, **p<0.01, ***p<0.001 compared with total mast cells in central airways. $^{\#\#}$p<0.01 compared with MC_{TC} in small airways. $^{¤}$p<0.05, $^{¤¤}$p<0.01 compared with MC_{TC} in central airways. Statistical analyses were performed using Mann-Whitney rank sum test.

Figure 6. Immunofluorescence micrographs exemplifying tryptase-positive mast cells co-positive for other selected mast cell related molecules. (A) IL-9R in small airways, (B) IgER1α in bronchi, (C) 5-LO in small airways, (D) renin in alveolar septa, (E) VEGF in pulmonary vessels and (F) LTC_4S in small airways. Mast cell tryptase is visualised with Alexa F 488 (green), and respective mast cell related molecule with Alexa F 555 (red). * denotes examples of co-positive cells which are also highlighted as insets. IgER1α (B) were visualised with DAB (brown) and the background tissue is outlined by DIC microscopy. In plates A, C-F, as background staining the autofluoroscence of extra cellular matrix fibres are visualised though blue UV light. Bar = 25 μm.

REFERENCES

1. Galli SJ, Kalesnikoff J, Grimbaldeston MA, *et al.* Mast cells as "tunable" effector and immunoregulatory cells: recent advances. *Annu Rev Immunol* 2005;23:749-86.

2. Gurish MF, Boyce JA. Mast cells: ontogeny, homing, and recruitment of a unique innate effector cell. *J Allergy Clin Immunol* 2006;117(6):1285-91.

3. Metcalfe DD, Baram D, Mekori YA. Mast cells. *Physiol Rev* 1997;77(4):1033-79.

4. Bradding P, Walls AF, Holgate ST. The role of the mast cell in the pathophysiology of asthma. *J Allergy Clin Immunol* 2006;117(6):1277-84.

5. Cai Y, Bjermer L, Halstensen TS. Bronchial mast cells are the dominating LTC4S-expressing cells in aspirin-tolerant asthma. *Am J Respir Cell Mol Biol* 2003;29(6):683-93.

6. Dawicki W, Marshall JS. New and emerging roles for mast cells in host defence. *Curr Opin Immunol* 2007;19(1):31-8.

7. Sayed BA, Christy A, Quirion MR, *et al.* The master switch: the role of mast cells in autoimmunity and tolerance. *Annu Rev Immunol* 2008;26:705-39.

8. Veerappan A, Reid AC, Estephan R, *et al.* Mast cell renin and a local renin-angiotensin system in the airway: role in bronchoconstriction. *Proc Natl Acad Sci U S A* 2008;105(4):1315-20.

9. Persson CG, Erjefalt JS, Korsgren M, *et al.* The mouse trap. *Trends Pharmacol Sci* 1997;18(12):465-7.

10. Kitamura Y. Heterogeneity of mast cells and phenotypic change between subpopulations. *Annu Rev Immunol* 1989;7:59-76.

11. Miller JS, Schwartz LB. Human mast cell proteases and mast cell heterogeneity. *Curr Opin Immunol* 1989;1(4):637-42.

12. Weidner N, Austen KF. Heterogeneity of mast cells at multiple body sites. Fluorescent determination of avidin binding and immunofluorescent determination of chymase, tryptase, and carboxypeptidase content. *Pathol Res Pract* 1993;189(2):156-62.

13. Irani AA, Schechter NM, Craig SS, *et al.* Two types of human mast cells that have distinct neutral protease compositions. *Proc Natl Acad Sci U S A* 1986;83(12):4464-8.

14. Balzar S, Chu HW, Strand M, *et al.* Relationship of small airway chymase-positive mast cells and lung function in severe asthma. *Am J Respir Crit Care Med* 2005;171(5):431-9.

15. Battaglia S, Mauad T, van Schadewijk AM, *et al.* Differential distribution of inflammatory cells in large and small airways in smokers. *J Clin Pathol* 2007;60(8):907-11.

16. Carroll NG, Mutavdzic S, James AL. Distribution and degranulation of airway mast cells in normal and asthmatic subjects. *Eur Respir J* 2002;19(5):879-85.

17. Brightling CE, Bradding P, Symon FA, *et al.* Mast-cell infiltration of airway smooth muscle in asthma. *N Engl J Med* 2002;346(22):1699-705.

18. Baraldo S, Turato G, Badin C, *et al.* Neutrophilic infiltration within the airway smooth muscle in patients with COPD. *Thorax* 2004;59(4):308-12.

19. Grashoff WF, Sont JK, Sterk PJ, *et al.* Chronic obstructive pulmonary disease: role of bronchiolar mast cells and macrophages. *Am J Pathol* 1997;151(6):1785-90.

20. Howard C, Reed M. Unbiased Stereology. *Advanced methods, Garland Science/BIOS Scientific Publishers, Second edition* 2005.

21. Forssell J, Sideras P, Eriksson C, *et al.* Interleukin-2-inducible T cell kinase regulates mast cell degranulation and acute allergic responses. *Am J Respir Cell Mol Biol* 2005;32(6):511-20.

22. Bienstock J. An update on mast cell heterogeniety*. *The journal of Allergy and Clinical Immunology* 1987;81(5):763-69.

23. Oskeritzian CA, Zhao W, Min HK, *et al.* Surface CD88 functionally distinguishes the MCTC from the MCT type of human lung mast cell. *J Allergy Clin Immunol* 2005;115(6):1162-8.

24. Irani AM, Schwartz LB. Human mast cell heterogeneity. *Allergy Proc* 1994;15(6):303-8.

25. Balzar S, Strand M, Rhodes D, *et al.* IgE expression pattern in lung: relation to systemic IgE and asthma phenotypes. *J Allergy Clin Immunol* 2007;119(4):855-62.

26. Kennedy Norton S, Barnstein B, Brenzovich J, *et al.* IL-10 Suppresses Mast Cell IgE Receptor Expression and Signaling In Vitro and In Vivo. *J Immunol* 2008;180(5):2848-54.

27. Fischer M, Harvima IT, Carvalho RF, *et al.* Mast cell CD30 ligand is upregulated in cutaneous inflammation and mediates degranulation-independent chemokine secretion. *J Clin Invest* 2006;116(10):2748-56.

28. Feger F, Varadaradjalou S, Gao Z, *et al.* The role of mast cells in host defense and their subversion by bacterial pathogens. *Trends Immunol* 2002;23(3):151-8.

29. Liebler JM, Qu Z, Buckner B, *et al.* Fibroproliferation and mast cells in the acute respiratory distress syndrome. *Thorax* 1998;53(10):823-9.

30. Metz M, Maurer M. Mast cells--key effector cells in immune responses. *Trends Immunol* 2007;28(5):234-41.

31. Dvorak AM. Human mast cells. *Adv Anat Embryol Cell Biol* 1989;114:1-107.

32. Welle M. Development, significance, and heterogeneity of mast cells with particular regard to the mast cell-specific proteases chymase and tryptase. *J Leukoc Biol* 1997;61(3):233-45.

33. Weibel ER HCaOM. How much are there really? Why stereology is essential in lung morphometry. *J Appl Physiol* 2007;102:459-467.

34. Weibel E, Hsia C, Ochs M. How much are there really? Why stereology is essential in lung morphometry. *J Appl Physiol* 2007;102:459-467.

35. Kambe N, Hiramatsu H, Shimonaka M, *et al.* Development of both human connective tissue-type and mucosal-type mast cells in mice from hematopoietic stem cells with identical distribution pattern to human body. *Blood* 2004;103(3):860-7.

36. Schulman ES, Kagey-Sobotka A, MacGlashan DW, Jr., *et al.* Heterogeneity of human mast cells. *J Immunol* 1983;131(4):1936-41.

37. Siddiqui S, Hollins F, Saha S, *et al.* Inflammatory cell microlocalisation and airway dysfunction: cause and effect? *Eur Respir J* 2007;30(6):1043-56.

38. Ammit AJ BS, Johnson PR, Hughes JM, Armour CL, Black JL. Mast cell numbers are increased in the smooth muscle of human sensitized isolated bronchi. *Am J Respir Crit Care Med* 1997;155:1123–1129.

39. Ekberg-Jansson A, Amin K, Bake B, *et al.* Bronchial mucosal mast cells in asymptomatic smokers relation to structure, lung function and emphysema. *Respir Med* 2005;99(1):75-83.

40. Hsieh FH, Sharma P, Gibbons A, *et al.* Human airway epithelial cell determinants of survival and functional phenotype for primary human mast cells. *Proc Natl Acad Sci U S A* 2005;102(40):14380-5.

Figure 1

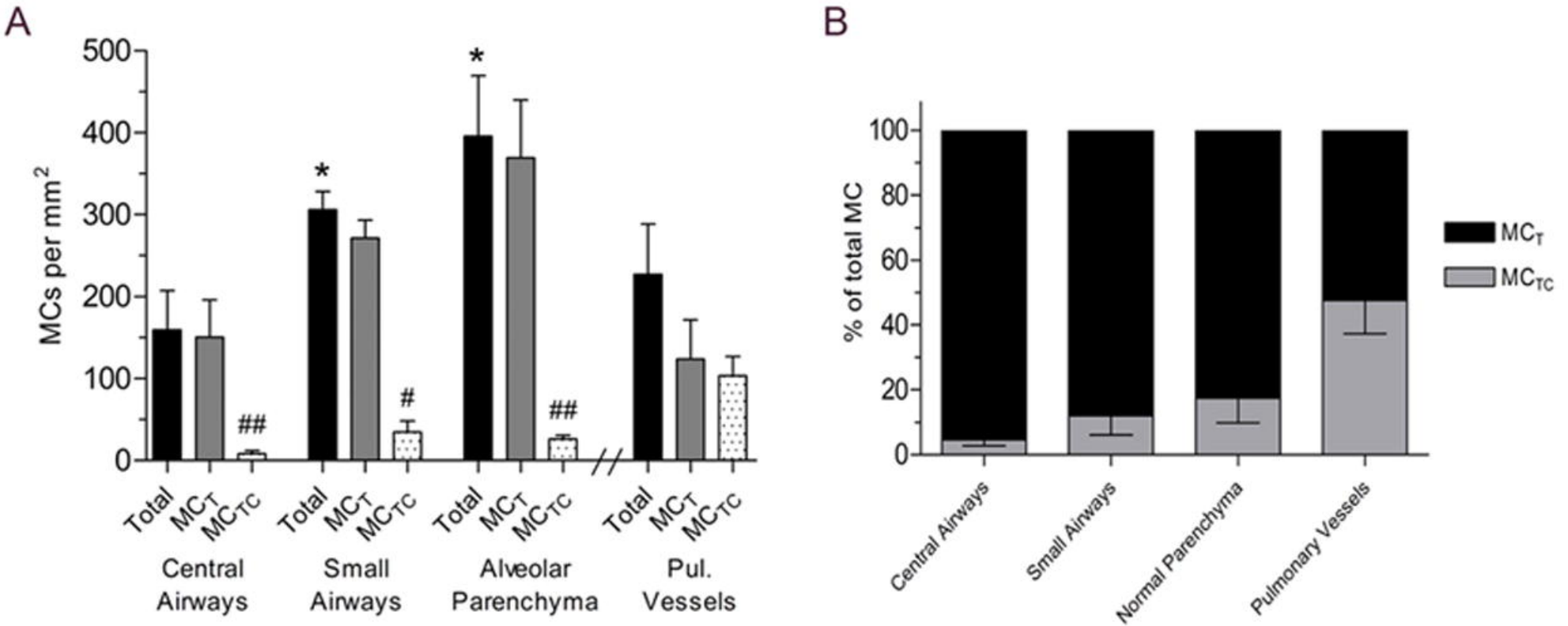
A
500
400
300
200
100
0
MCs per mm2
*
*
#
##
##
Total
MCT
MCTC
Central Airways
Small Airways
Alveolar Parenchyma
Pul. Vessels
B
100
80
60
40
20
0
% of total MC
MCT
MCTC
Central Airways
Small Airways
Normal Parenchyma
Pulmonary Vessels

Figure 2

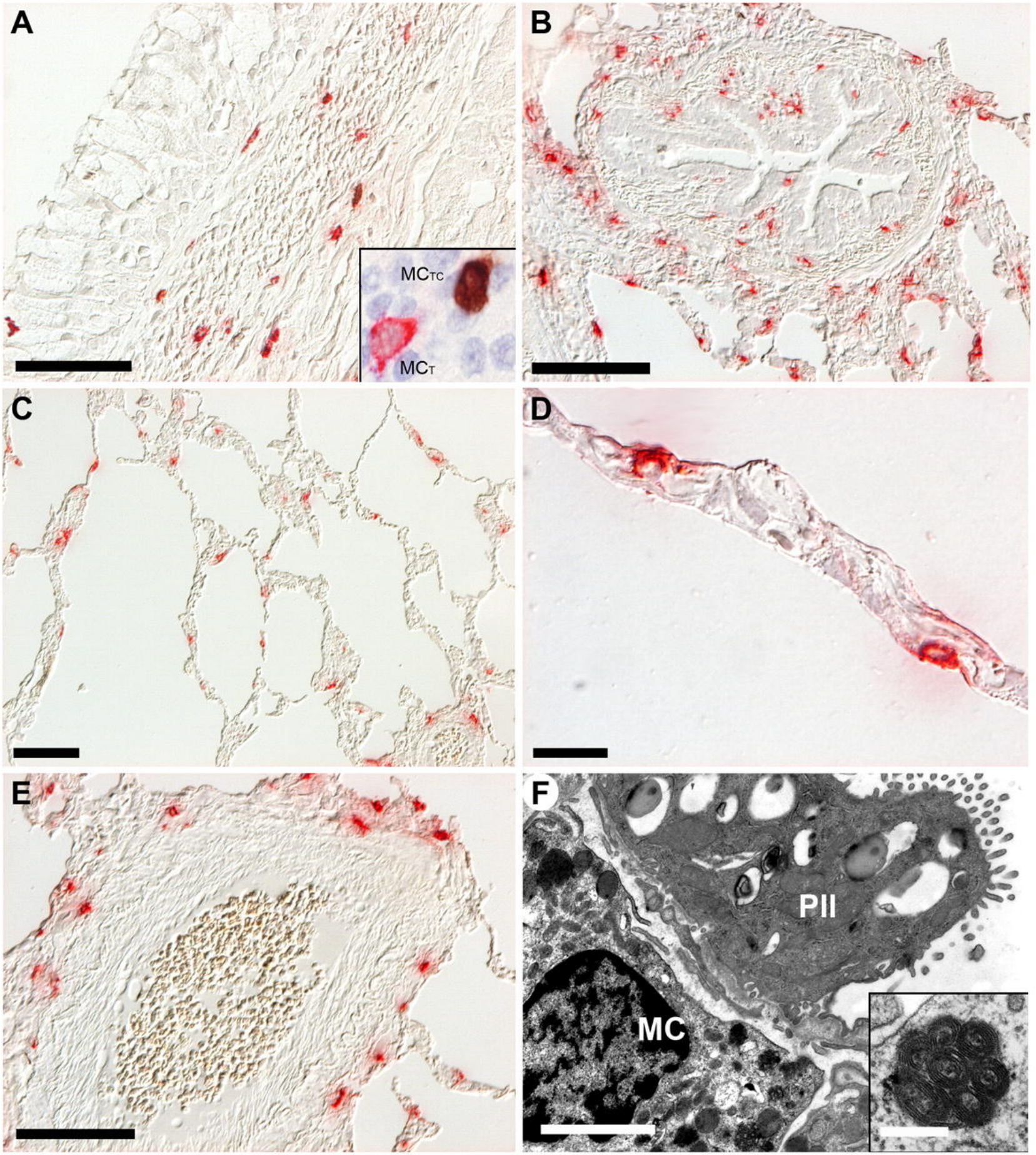

Figure 3

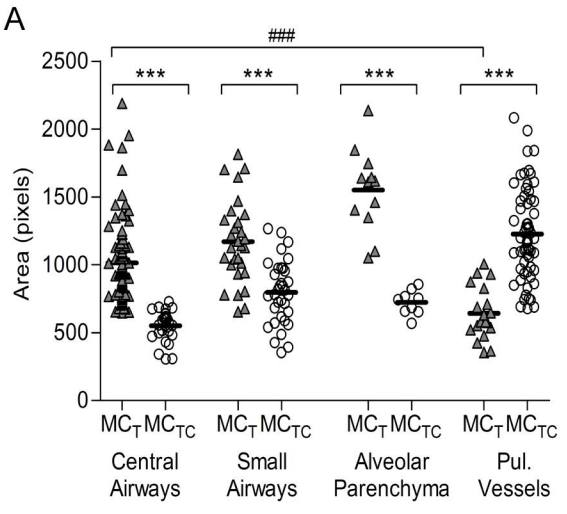
A
###
***
***
***
***
2500
2000
1500
1000
500
0
Area (pixels)
MC_T MC_TC
MC_T MC_TC
MC_T MC_TC
MC_T MC_TC
Central Airways
Small Airways
Alveolar Parenchyma
Pul. Vessels

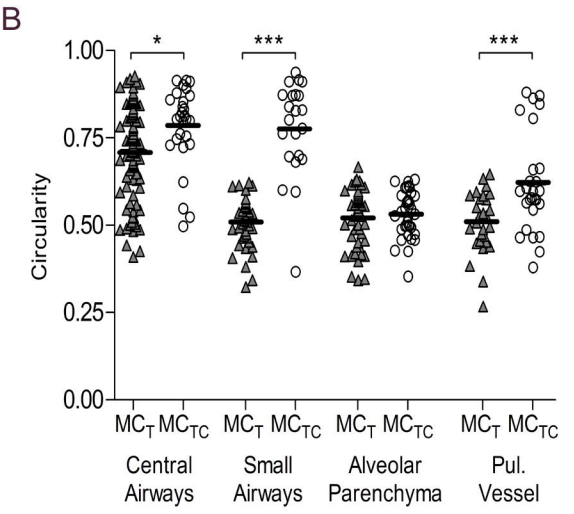
B
*
***
***
1.00
0.75
0.50
0.25
0.00
Circularity
MC_T MC_TC
MC_T MC_TC
MC_T MC_TC
MC_T MC_TC
Central Airways
Small Airways
Alveolar Parenchyma
Pul. Vessel

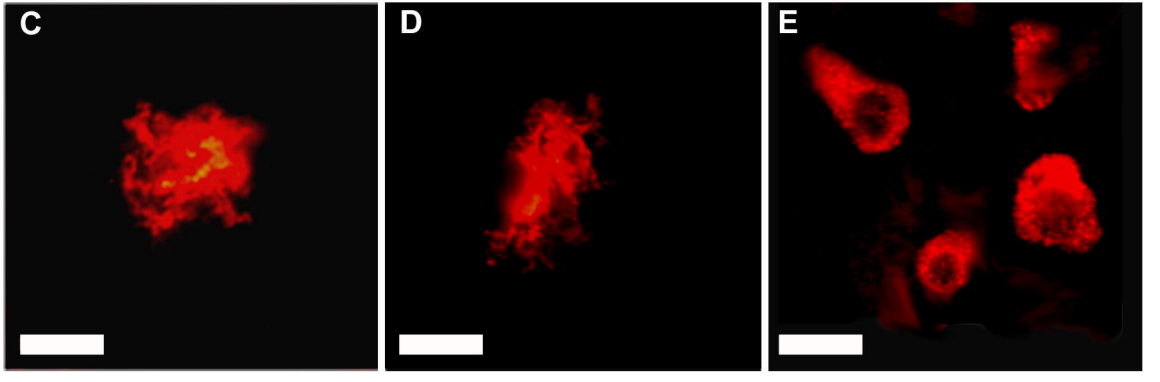
C
D
E

Figure 4

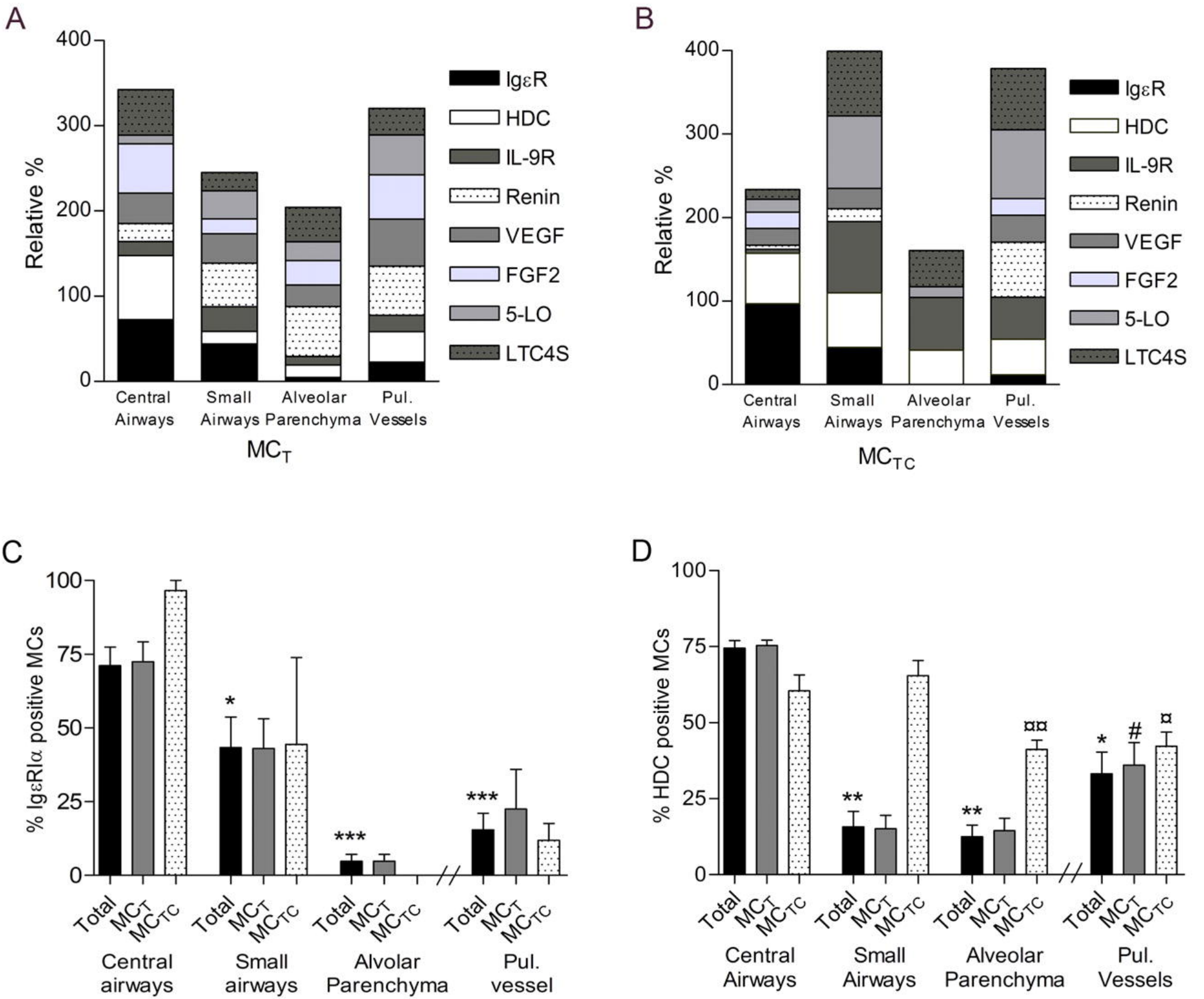
A
400
300
200
100
0
Relative %
IgεR
HDC
IL-9R
Renin
VEGF
FGF2
5-LO
LTC4S
Central Airways
Small Airways
Alveolar Parenchyma
Pul. Vessels
MCT
B
400
300
200
100
0
Relative %
IgεR
HDC
IL-9R
Renin
VEGF
FGF2
5-LO
LTC4S
Central Airways
Small Airways
Alveolar Parenchyma
Pul. Vessels
MCTC
C
100
75
50
25
0
% IgεRIα positive MCs
*
***
***
Total
MCT
MCTC
Central airways
Small airways
Alvolar Parenchyma
Pul. vessel
D
100
75
50
25
0
% HDC positive MCs
**
**
¤¤
*
#
¤
Total
MCT
MCTC
Central Airways
Small Airways
Alveolar Parenchyma
Pul. Vessels

Figure 5

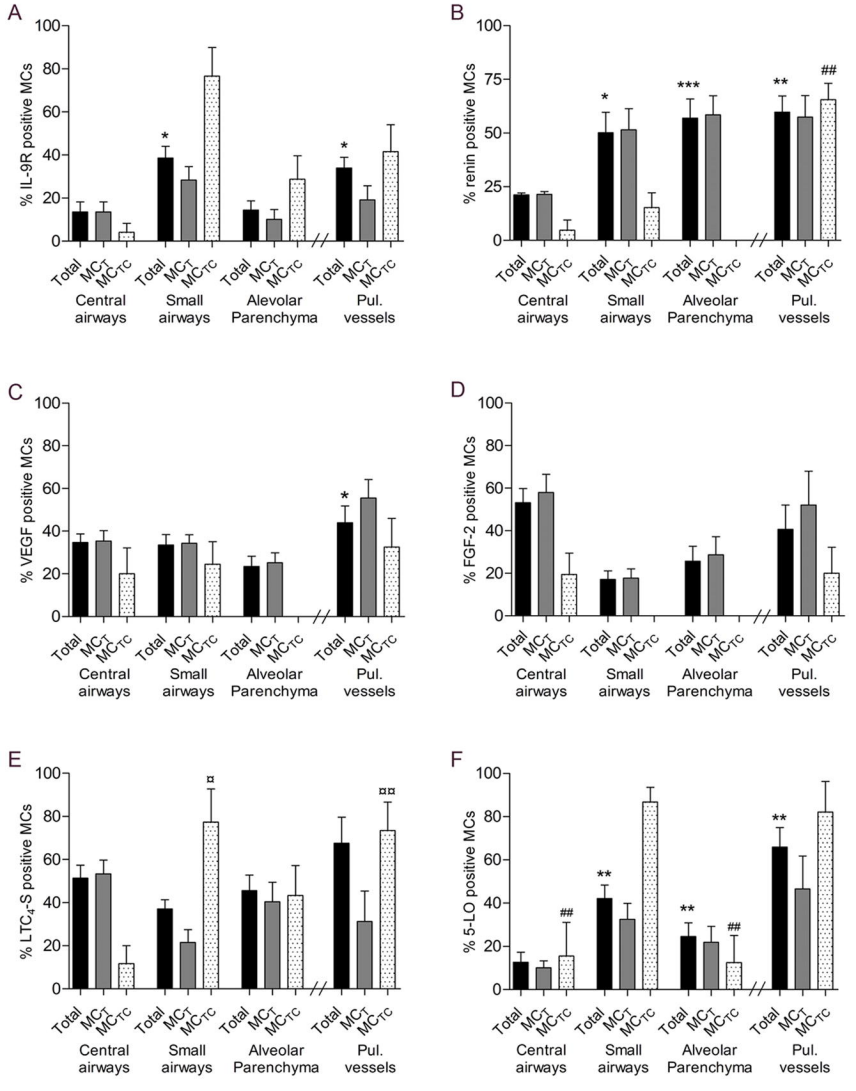
A
% IL-9R positive MCs
100
80
60
40
20
0
*
*
Total
MCT
MCTC
Central airways
Small airways
Alvelolar Parenchyma
Pul. vessels
B
% renin positive MCs
100
75
50
25
0
*
***
**
##
C
% VEGF positive MCs
*
D
% FGF-2 positive MCs
E
% LTC4-S positive MCs
¤
¤¤
F
% 5-LO positive MCs
**
**
**
##
##

Figure 6

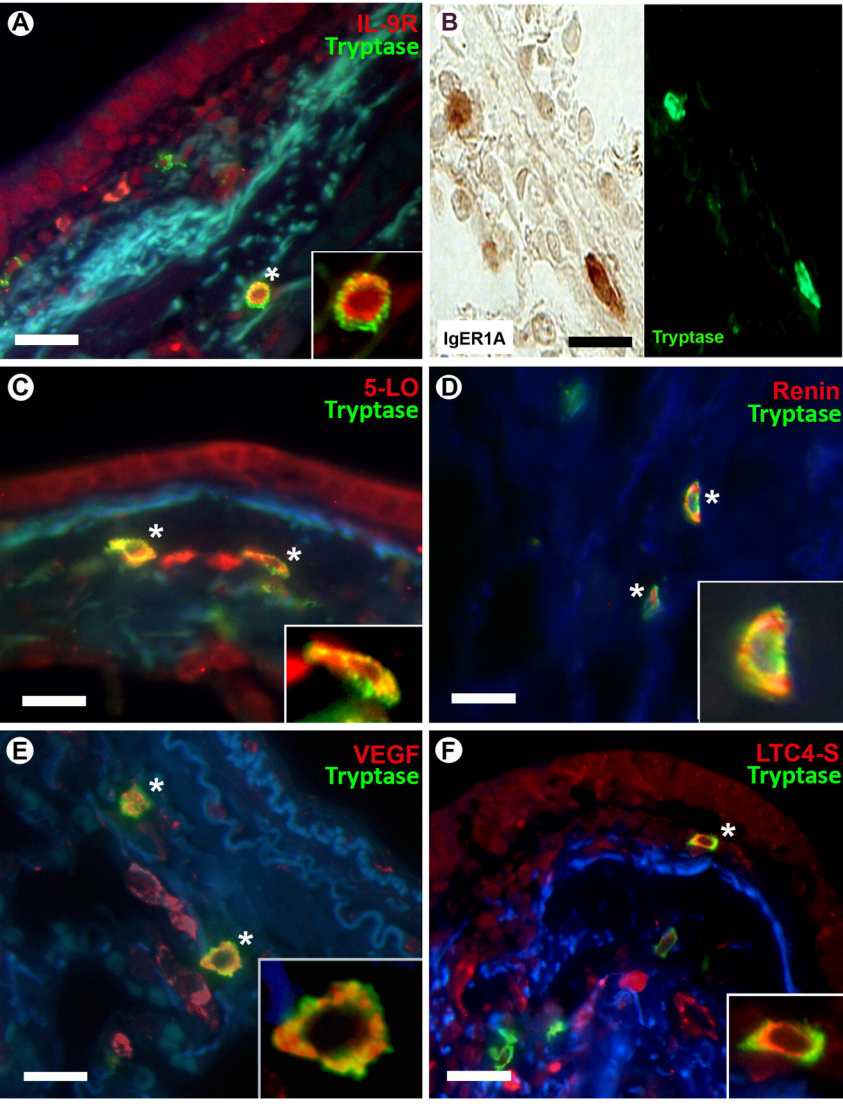
A
IL-9R
Tryptase
B
IgER1A
Tryptase
C
5-LO
Tryptase
D
Renin
Tryptase
E
VEGF
Tryptase
F
LTC4-S
Tryptase

ONLINE SUPPLEMENTARY DATA

METHODS

Lung resections

Ten non-smoking patients (mean age 62 yrs) undergoing surgery for suspected lung cancer at Lund University Hospital was included in the study. Only patients with solid, well defined tumors were included, and tissue was obtained as far from the tumor as possible (table 1). Patients had no symptoms of infections at least four weeks prior to the beginning of the study and none were treated with oral or inhaled steroids. Already at the operating theatre multiple tissue slices (around 15 mm thick) from regions far from the tumor were put aside and immediately immersed in fixative. After fixation overnight the tissue were trimmed into blocks with aim to get blocks for paraffin embedding that contained most anatomical regions of the lungs.

Tissue processing

After fixations (4% formalin in phosphate buffer, pH 7.2) tissue blocks were dehydrated through a series of increasing ethanol solutions, cleared in xylene and embedded in paraffin. From each block a large number of sequential sections of 3µm thickness were generated using a HM 350 SV microtome (Microme International, Walldorf, Germany).

Double IHC staining of MC_T and MC_{TC}

To stain for mast cell subtypes, mucosal mast cells (MC_T, positive for the protease tryptase) and connective tissue mast cells (MC_{TC}, positive for proteases chymase and tryptase), a double staining technique was developed using the fact that all mast cells have tryptase. By saturating all chymase positive mast cells with a dark brown DAB (3,3'-diaminobenzidine)

precipitation staining they become inert to further mast cell tryptase staining (the precipitated DAB complex constitutes a steric hindrance for any further antibody binding). Hence, by subsequent use of a direct alkaline phosphatase (AP) conjugated anti-MC tryptase antibody, only mucosal mast cells are receptive for red staining with AP substrate Fuchsin. In running this protocol paraffin sections were pre-treated with high temperature antigen unmasking technique (microwave, citrate buffer, pH 6, for 2x7 min, 800W). Sections were blocked for endogenous peroxidase with 0.3% H_2O_2 in 10% methanol for 30 minutes in room temperature, and blocked for unspecific binding in 5 % normal goat serum. Sections were incubated with primary antibody, mouse monoclonal anti-MC chymase (see table 2) overnight in 4°C and with peroxide conjugated goat-anti mouse secondary antibody (see table 2) for 1 hour in room temperature, and developed using DAB Substrate Kit (SK-4100, Vector Laboratories, Burlingame, CA, USA) according to manufactures direction. Next, sections were incubated with AP-conjugated mouse monoclonal anti-MC tryptase (see table 2) for 1 hour in room temperature followed by development with Fuchsin+ Substrate-Chromogen System (K0625, Dako, Glostrup, Denmark), according to manufacturers direction. Background staining was visualized with heamatoxylin and sections were mounted in Kaisers mounting medium (Merck, Darmstadt, Germany). The resulting staining was dark brown MC_{TC} cells whereas the MC_T population appeared bright red.

Density analysis

The densities (cells per μm^2 tissue area) of MC_T and MC_{TC} were calculated in the walls of bronchi and small airways, pulmonary vessels, as well as in the alveolar lung parenchyma and pleural wall. In each tissue region a large number of cells were quantified and related to the analyzed tissue area. The alveolar tissue area was calculated by image analysis (Image-pro plus, MediaCybernetics, Inc., USA and NIS-elements, Nikon, USA) so that only the firm tis-

sue (i.e. the alveolar septa) was measured. The approach of excluding airspaces thus gives a more relevant tissue density in this compartment. Small patchy regions of microscopic emphysema, occasional patchy areas of microscopic fibrotic lesions were also found and included in the analysis. We also calculated the proportion of MC_T and MC_{TC} in subregions of bronchi/bronchioles (*epithelium, lamina propria, smooth muscle* and *adventitia*) and the distinct regions of pulmonary vessels (*intima, media* and *adventitia*).

Immunohistochemical identification of mast cell-related molecules

Paraffin sections were blocked for unspecific binding in 5 % dry milk mixed with 20% normal horse/goat/donkey serum (Vector Laboratories, Burlingame, CA) in ambient temperature for 30 min. Sections were blocked for endogenous streptavidin and biotin with avidin/biotin blocking kit (Vector Laboratories, Burlingame, CA, USA). After appropriate antigen retrieval the sections were incubated with primary antibodies of the molecules of interest (dilutions are presented in table 2) . All antibodies have been tested and validated for immunohistochemical use on formalin-fixed tissues and paraffin sections: IL-9 receptor [1], vascular endothelial growth factor [2], 5 lipoxygenase [3], leukotriene C4 synthase [4], renin [5], fibroblast growth factor 2 [6], histidine decarboxylase [7], c-kit [8], see also table 2) After a rinse step sections were incubated for 1 hour in ambient temperature with the biotinylated secondary antibody (see table 2). Next, sections were incubated with Alexa Flour 555-conjugated streptavidin (1:200, 10 µg/ml, S21381, Molecular Probes, OR, USA) for 30 minutes in ambient temperature. To stain the same sections also for mast cell subtypes (MC_T and MC_{TC}) mouse monoclonal antibodies, used in the double staining described above, anti-MC tryptase and anti-MC chymase, were directly labeled with Alexa Fluor 488 and Alexa Fluor 350, respectively, using Zenon® Mouse IgG labelling kit (Invitrogen, Molecular probes, USA). Sections were incubated with the mixed solutions for 1 hour in ambient temperature and mounted in Vectashield mounting

medium (H-1000, Vector Laboratories, Burlingame, CA). All rinse steps were in TBS buffer. The microscopic examination was performed on a Nikon 80i fluorescence microscope equipped with multiple wave-length specific UV filters.

Transmission electron microscopy

After fixation in buffer supplemented with 1% glutaraldehyde and 3% formaldehyde over-night the samples were rinsed in buffer, post fixed in 1% osmium tetroxide for 1 h, and dehydrated in graded acetone solutions and embedded in Polarbed 812. One μm thick plastic sections were examined by bright field microscopy and areas with a well preserved morphology were selected for electron microscopic analysis. Ultrathin sections (90 nm) were cut and placed on 200-mesh, thin bar copper grid before staining with uranyl acetate and lead citrate [9]. The specimens were examined on a Philips CM-10 transmission electron microscope (Philips, Netherlands). MC_T and MC_{TC}, were analyzed according to criteria stated by Dvorak in 2005 [10].

RESULTS

Proportion and distribution of MC_T and MC_{TC}

The detailed distribution of mast cells was further investigated in sub-anatomical compartments within small airways, pulmonary vessels and alveoli (supplementary fig 1A-B). In summary, in small airways a relative accumulation of MC_{TC} was found in the smooth muscle whereas this subtype was absent in the epithelium (fig 1A). In pulmonary vessels both mast cell subtypes displayed a similar distribution with the exception of the smooth muscle-rich media where only MC_{TC} were found (fig 1B). In the alveolar region the mast cells were evenly distributed within alveolar septa with no detectable mast cells in the alveolar lumen.

Transmission electron microscopy corroborated a strict interstitial distribution among alveolar mast cells.

The distinct sizes of MC_T and MC_{TC} are independent of tissue sectional planes.

Similar distinct size differences were present in longitudinally sectioned small airways (MC_T 1162±25 and MC_{TC} 616±15) and pulmonary vessels (MC_T 578±20 and MC_{TC} 1247±48) (Fig 2) as observed in the cross sectioned material.

REFERENCES

1. Demoulin JB, Uyttenhove C, Van Roost E, *et al.* A single tyrosine of the interleukin-9 (IL-9) receptor is required for STAT activation, antiapoptotic activity, and growth regulation by IL-9. *Mol Cell Biol* 1996;16(9):4710-6.
2. de Paulis A, Prevete N, Fiorentino I, *et al.* Expression and functions of the vascular endothelial growth factors and their receptors in human basophils. *J Immunol* 2006;177(10):7322-31.
3. Woods JW. 5-Lipoxygenase is located in the euchromatin of the nucleus in resting human alveolar macrophages and translocates to the nuclear envelope upon cell activation. *J. Clin. Invest.* 1995;95:2035-2046.
4. Cai Y, Bjermer L, Halstensen TS. Bronchial mast cells are the dominating LTC4S-expressing cells in aspirin-tolerant asthma. *Am J Respir Cell Mol Biol* 2003;29(6):683-93.
5. Silver RB, Reid AC, Mackins CJ, *et al.* Mast cells: a unique source of renin. *Proc Natl Acad Sci U S A* 2004;101(37):13607-12.
6. Jensen L, Bangsbo J, Hellsten Y. Effect of high intensity training on capillarization and presence of angiogenic factors in human skeletal muscle. *J Physiol* 2004;557(Pt 2):571-82.
7. Dartsch C, Sundler F, Persson L. Antisera against rat recombinant histidine decarboxylase: immunocytochemical studies in different species. *Histochem J* 1999;31(8):507-14.
8. Tsuura Y, Hiraki H, Watanabe K, *et al.* Preferential localization of c-kit product in tissue mast cells, basal cells of skin, epithelial cells of breast, small cell lung carcinoma and seminoma/dysgerminoma in human: immunohistochemical study on formalin-fixed, paraffin-embedded tissues. *Virchows Arch* 1994;424(2):135-41.
9. Erjefalt JS, Sundler F, Persson CG. Eosinophils, neutrophils, and venular gaps in the airway mucosa at epithelial removal-restitution. *Am J Respir Crit Care Med* 1996;153(5):1666-74.
10. Forssell J, Sideras P, Eriksson C, *et al.* Interleukin-2-inducible T cell kinase regulates mast cell degranulation and acute allergic responses. *Am J Respir Cell Mol Biol* 2005;32(6):511-20.

Figure 1.

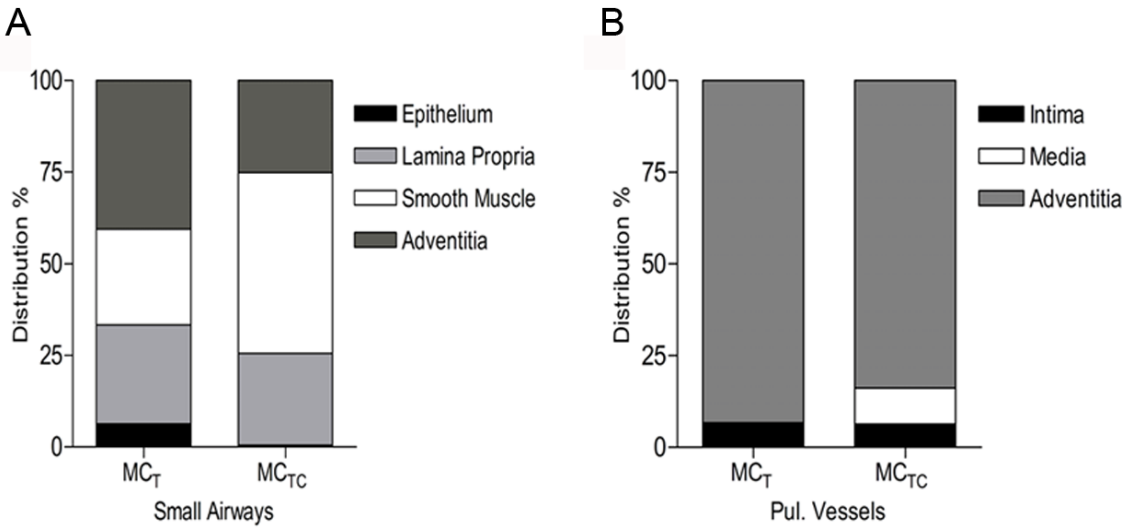

Figure 2.

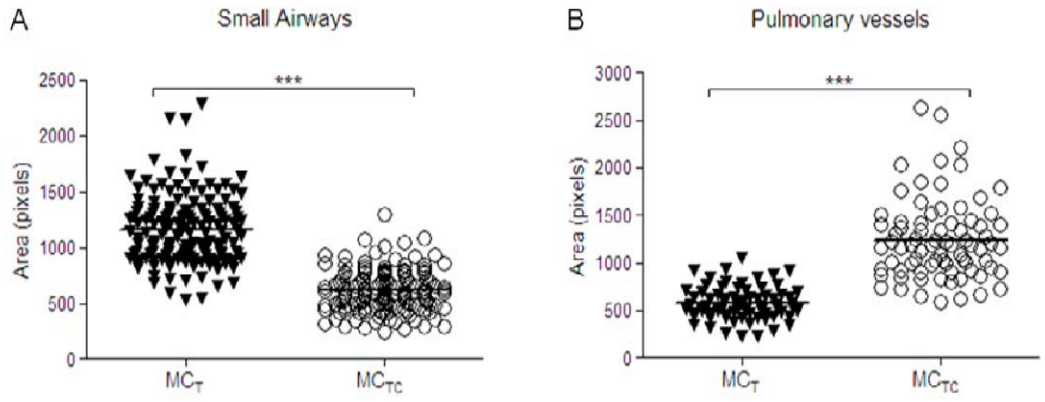

LEGENDS

Figure 1

Illustration of the detailed localization in % of mast cell subtypes in small airway epithelium lamina propria, smooth muscle and adventitia (A) and pulmonary vessel intima, media and adventitia (B).

Figure 2

Mast cell size in longitudinally sectioned small airways (A) and pulmonary vessels (B) in the cross sectioned material stained for c-kit. Results are shown as scatter plot graphs were black bar indicates mean. Statistical analyses were performed using Mann-Whitney rank sum test. ***$p<0.001$ when comparing MC_T and MC_{TC} size in different anatomical locations.